

Abnormal Spontaneous Blood Oxygenation Level Dependent Fluctuations in Children with Focal Cortical Dysplasias

Citation for published version (APA):

Dangouloff-Ros, V., Jansen, J., De Jong, J., Postma, A. A., Hoeberigs, C., Fillon, L., Boisgontier, J., Roux, C.-J., Levy, R., Varlet, P., Blauwblomme, T., Eisermann, M., Losito, E., Bourgeois, M., Chiron, C., Nabbout, R., Boddaert, N., & Backes, W. (2023). Abnormal Spontaneous Blood Oxygenation Level Dependent Fluctuations in Children with Focal Cortical Dysplasias: Initial findings in surgically confirmed cases. *Neuropediatrics*, 54(3), 188-196. <https://doi.org/10.1055/a-1959-9241>

Document status and date:

Published: 01/06/2023

DOI:

[10.1055/a-1959-9241](https://doi.org/10.1055/a-1959-9241)

Document Version:

Publisher's PDF, also known as Version of record

Document license:

Taverne

Please check the document version of this publication:

- A submitted manuscript is the version of the article upon submission and before peer-review. There can be important differences between the submitted version and the official published version of record. People interested in the research are advised to contact the author for the final version of the publication, or visit the DOI to the publisher's website.
- The final author version and the galley proof are versions of the publication after peer review.
- The final published version features the final layout of the paper including the volume, issue and page numbers.

[Link to publication](#)

General rights

Copyright and moral rights for the publications made accessible in the public portal are retained by the authors and/or other copyright owners and it is a condition of accessing publications that users recognise and abide by the legal requirements associated with these rights.

- Users may download and print one copy of any publication from the public portal for the purpose of private study or research.
- You may not further distribute the material or use it for any profit-making activity or commercial gain
- You may freely distribute the URL identifying the publication in the public portal.

If the publication is distributed under the terms of Article 25fa of the Dutch Copyright Act, indicated by the "Taverne" license above, please follow below link for the End User Agreement:

www.umlib.nl/taverne-license


Take down policy

If you believe that this document breaches copyright please contact us at:

repository@maastrichtuniversity.nl

providing details and we will investigate your claim.

Abnormal Spontaneous Blood Oxygenation Level Dependent Fluctuations in Children with Focal Cortical Dysplasias: Initial Findings in Surgically Confirmed Cases

Volodia Dangouloff-Ros^{1,2,3,4,5}  Jacobus F.A. Jansen^{4,5} Joost de Jong^{4,5} Alida A. Postma^{4,5}
 Christianne Hoerberigs⁴ Ludovic Fillon^{1,2,3} Jennifer Boisgontier^{1,2,3} Charles-Joris Roux^{1,2,3}
 Raphael Levy^{1,2,3} Pascale Varlet⁶ Thomas Blauwblomme^{7,8} Monika Eisermann^{8,9} Emma Losito^{8,10}
 Marie Bourgeois⁷ Catherine Chiron^{8,10,11} Rima Nabbout^{8,10} Nathalie Boddaert^{1,2,3}
 Walter Backes^{4,5}

¹ Pediatric Radiology Department, AP-HP, Hôpital Universitaire Necker-Enfants Malades, Paris, France

² Université de Paris, INSERM U1199, Paris, France

³ Université de Paris, Institut Imagine, Paris, France

⁴ Department of Radiology, Maastricht University Medical Center, Maastricht, the Netherlands

⁵ School of Mental Health and Neurosciences, Maastricht, the Netherlands

⁶ Neuropathology Department, GHU Paris, Université de Paris, 1 rue Cabanis, Paris

⁷ Pediatric Neurosurgery Department, AP-HP, Hôpital Universitaire Necker-Enfants Malades, Paris, France

⁸ Université de Paris, INSERM U1129, Pediatric Epilepsies and Brain Plasticity, Paris, France

Address for correspondence Volodia Dangouloff-Ros, MD, MSc, Department of Pediatric Radiology, Assistance-Publique Hôpitaux de Paris, Hôpital Universitaire Necker-Enfants Malades, 149 rue de Sèvres, 75015 Paris, France (e-mail: volodia.dangouloff-ros@aphp.fr).

⁹ Department of Clinical Neurophysiology, Hôpital Universitaire Necker-Enfants Malades, Paris, France

¹⁰ Pediatric Neurology Department, Reference Center for Rare Epilepsies, Hôpital Universitaire Necker-Enfants Malades, Paris, France

¹¹ Department of Nuclear Medicine, SHFJ-CEA, Orsay, France

Neuropediatrics 2023;54:188–196.

Abstract

Keywords

- ▶ malformation of cortical development
- ▶ functional MRI
- ▶ children
- ▶ epilepsy
- ▶ seizures

Background Focal cortical dysplasias (FCD) are a frequent cause of drug-resistant epilepsy in children but are often undetected on structural magnetic resonance imaging (MRI). We aimed to measure and validate the variation of resting state functional MRI (rs-fMRI) blood oxygenation level dependent (BOLD) metrics in surgically proven FCDs in children, to assess the potential yield for detecting and understanding these lesions.

Methods We prospectively included pediatric patients with surgically proven FCD with inconclusive structural MRI and healthy controls, who underwent a ten-minute rs-fMRI acquired at 3T. Rs-fMRI data was pre-processed and maps of values of regional homogeneity (ReHo), degree centrality (DC), amplitude of low frequency fluctuations (ALFF) and fractional ALFF (fALFF) were calculated. The variations of BOLD metrics within the to-be-resected areas were analyzed visually, and quantitatively using lateralization indices. BOLD metrics variations were also analyzed in fluorodeoxyglucose-positron emission tomography (FDG-PET) hypometabolic areas.

received

May 17, 2022

accepted after revision

October 7, 2022

accepted manuscript online

October 12, 2022

article published online

December 27, 2022

© 2022. Thieme. All rights reserved.

Georg Thieme Verlag KG,

Rüdigerstraße 14,

70469 Stuttgart, Germany

DOI <https://doi.org/10.1055/a-1959-9241>.

ISSN 0174-304X.

Results We included 7 patients (range: 3–15 years) and 6 aged-matched controls (range: 6–17 years). ReHo lateralization indices were positive in the to-be-resected areas in 4/7 patients, and in 6/7 patients in the additional PET hypometabolic areas. These indices were significantly higher compared to controls in 3/7 and 4/7 patients, respectively. Visual analysis revealed a good spatial correlation between high ReHo areas and MRI structural abnormalities (when present) or PET hypometabolic areas. No consistent variation was seen using DC, ALFF, or fALFF.

Conclusion Resting-state fMRI metrics, noticeably increase in ReHo, may have potential to help detect MRI-negative FCDs in combination with other morphological and functional techniques, used in clinical practice and epilepsy-surgery screening.

Introduction

Focal cortical dysplasias (FCDs) are defined by a disorganization of cortical lamination.¹ They are the main cause of lesional focal childhood epilepsy, which is most commonly drug-resistant.^{1,2} FCDs may be seen on structural magnetic resonance imaging (MRI) as abnormal sulcus, cortical thickening, blurring of the gray matter–white matter junction, signal abnormality between the germinal matrix and the (abnormal) cortex.¹ However, they are invisible on MRI in 13 to 25% of surgically proven cases,^{3,4} more frequently in type I than in type II.³ These numbers are thought to be higher when FCDs, that are not resected, are added.

The exploration of MRI-negative FCDs is a major clinical topic, which can drastically change the management of the epilepsy in these children.^{1,5} Indeed, the absence of an abnormality on MRI is associated with worse surgical outcome.⁶ Several techniques are already available, from electrophysiological exploration (scalp electroencephalography and intracranial electroencephalography) to functional imaging such as positron emission tomography (PET). PET, most frequently using fluorodeoxyglucose (FDG), usually shows a hypometabolism of the FCD area during interictal period.⁷ This noninvasive functional imaging technique greatly improved diagnostic workup, but no technique provides a perfect detection rate, and the detection of FCDs still relies on a multimodal approach. In this context, new functional techniques that could reflect physiological abnormalities would be of interest to improve our ability to detect and understand FCDs.

Boerwinkle et al reported that independent component analysis of resting-state functional MRI (fMRI) networks allows a good detection of seizure onset zones, even in MRI-negative patients.^{8,9} Resting-state fMRI also allows computation of metrics reflecting several characteristics of spontaneous blood oxygenation level dependent (BOLD) signal fluctuations locally, thus voxel-wise in relation to surrounding voxels. Among these, four physiological metrics are of interest: (i) regional homogeneity (ReHo),¹⁰ (ii) amplitude of low-frequency fluctuations (ALFF) and (iii) fractional ALFF (fALFF),¹¹ and (iv) degree centrality (DC).¹² Gupta et al reported previously higher ReHo and lower fALFF in adult patients with FCD, but this was based on morphologically visible FCDs,¹³ whereas Chen et al reported that ReHo was

helpful to detect several types of malformations of cortical development.¹⁴

Our goal was to prospectively analyze whether MRI-negative (or inconclusive MRI) surgically proven FCDs in children display quantitative asymmetries of the resting-state images, which could help to detect and characterize these epileptogenic lesions.

Materials and Methods

This work has been carried out in accordance with The Code of Ethics of the World Medical Association (Declaration of Helsinki) for experiments involving humans. This study was approved by the local ethical committee (CPP Est 1, 2017-32-2016-A0207546) and all subjects (according to their age) and their parents gave their written informed consent prior to participation.

Patients

From January 2016 to February 2019, we prospectively included patients according to the following criteria: (1) age under 18 years old; (2) drug-resistant focal epilepsy, likely related to an FCD; (3) no or inconclusive abnormality seen on a first MRI; (4) surgical project to cure the epilepsy (based on the multidisciplinary evaluation by our children epilepsy-dedicated center). After this first step, they had fMRI and PET (see below), and if the FCD was not clearly delineated using PET and electroclinical data, they had intracranial stereo-electroencephalography to delineate the seizure onset zone. Then, if the surgical resection was deemed feasible and accepted by the parents, they were included in the analysis if FCD was confirmed on histopathological sample. Patients were excluded if the surgical specimen displayed no FCD or if the fMRI images were impossible to analyze due to head movement artifacts even after motion correction (incidental movements stronger than 6 mm).

For comparison, we also included healthy pediatric controls, who attended mainstream education and were screened for neuropsychological and motor problems, presenting no cognitive or motor impairments.

Imaging

As a part of their presurgical workup, patients underwent a structural MRI examination on a 3T MR scanner, including

three-dimensional (3D) T1-weighted (T1w) images, 3D fluid attenuated inversion recovery, transverse and coronal T2-weighted images, and susceptibility weighted imaging. Additionally, they underwent a resting-state fMRI BOLD sequence with following parameters: single shot echo planar imaging sequence; TE/TR 31/2500ms; $2 \times 2 \text{ mm}^2$ pixel size, 3-mm thick adjacent transverse slices covering the entire cerebrum and cerebellum (45 slices); 240 dynamics; and acquisition time 10 min. Simultaneous electroencephalogram (EEG) was recorded during the MRI, allowing to check if patients were sleeping or not.

Separately from the MRI, 3D PET-CT images were obtained using ECAT EXACT HR. Images were acquired for 15 to 20 minutes starting 30 minutes after intravenous injection of 3.7 mBq/kg of ^{18}F -FDG. Attenuation-corrected data were reconstructed into 89 transversal slices, with a resulting resolution of 5 mm full width at half maximum. For one patient, PET images were obtained using SIGNA PET/MR. Images were acquired for 30 minutes starting 30 minutes after intravenous injection of 3.7 mBq/kg of ^{18}F -FDG. Attenuation-corrected data were reconstructed into 89 transversal slices, with a resulting resolution of 2.78 mm full width at half maximum.

Controls had the same imaging protocol, without the PET-CT images.

Functional MR Image Processing

The processing was performed using automated software (DPARSF (<http://rfmri.org/DPARSF>)¹⁵, which is based on statistical parametric mapping (SPM12, <http://www.fil.ion.ucl.ac.uk/spm>) and the toolboxes Resting-State Functional MR imaging Toolkit (REST; <http://www.restfmri.net>)¹⁶ and Data Processing & Analysis for (Resting-State) Brain Imaging (DPABI, <http://rfmri.org/DPABI>)¹⁷).

After removal of the images pertaining to the first 10 seconds to account for magnetic stabilization, the functional images were slice-time and motion corrected and affinely co-registered to the anatomical 3D T1-weighted images. Any signal drifts were corrected by removing the very low frequency components ($<0.01 \text{ Hz}$). To correct for physiological fluctuations, averaged time series from the cerebrospinal fluid and white matter were included as covariates in the linear regression analysis.

Kendall's coefficient of concordance was calculated to determine ReHo of the time-series of a given voxel with its 26 surrounding voxels.¹⁰ To obtain the ALFF, the time series were converted to the frequency domain by means of fast Fourier transform to obtain the power spectrum. Then, the power spectrum was square-rooted and averaged over the 0.01 to 0.1 Hz frequency range for each voxel.¹¹ Fractional ALFF was defined as the ratio of total amplitude within the low-frequency range (0.01–0.1 Hz) to the total amplitude of the entire detectable frequency range.¹⁵ To calculate DC, a correlation matrix was firstly obtained by computing Pearson correlation (r) coefficients between the time series of one voxel with all other voxel time series¹² within a predefined gray matter mask with gray matter probabilities greater than 20%. An undirected adjacency matrix was then obtained by

thresholding each correlation at $r > 0.25$ to remove the weak correlations strongly influenced by noise. Then, the weighted DC was computed as the sum of the weight of the significant connections between a given voxel and all other voxels.¹⁸

Image Analysis

Structural images were reviewed in consensus by two pediatric neuroradiologists (*_blinded for review_*, 25 years of experience in pediatric epilepsy imaging and *_blinded for review_*, 8 years of experience), to look for previously unseen abnormalities, in particular in the to-be-resected area.

The surgically resected area including histopathologically confirmed FCD was used as a gold standard to delineate lesional area (even if the FCD may be larger or smaller than the resected area). Preoperative and postoperative MRI, as well as PET images, were spatially coregistered to delineate manually 3D regions of interest (ROI) corresponding to the resected areas. Resected/remaining sulci were visually checked to correct for possible brain shift after surgery. Contralateral ROIs were manually delineated to include the corresponding sulci. These ROI masks were then registered to the gray matter segmentation map (obtained using FreeSurfer software Version 5.3.0; <http://surfer.nmr.mgh.harvard.edu>) and to the functional maps in order to extract the values of each of the BOLD measures (and PET standardized uptake value [SUV]) in only the gray matter part of the ROI. Gray matter was used because it provides the highest BOLD contrast to noise ratio.¹⁹

To allow comparison with controls, the same ROIs were manually duplicated on every control (i.e., for each control as many ROIs as the number of included patients).

As a secondary analysis, PET images were also analyzed by an experienced reader (*_blinded for review_*) to draw ROIs of the lowest metabolism (suspected FCD) in the same lobe as the proven FCD.

Visual analysis of BOLD metrics or PET maps was done by overlaying spatially registered maps on 3D T1w images with delineation of the surgical ROI. The correspondence of anatomical boundaries of surgical ROIs and areas of focal BOLD metric or PET abnormality was defined as: (1) full colocalization, when the areas matched fully; (2) larger surgical ROI, when focal BOLD/PET abnormality was found within a larger surgical ROI; (3) larger BOLD/PET abnormality, when the focal abnormality overlapped the surgical ROI and the surrounding brain; (4) inconclusive, when no clear focal BOLD/PET asymmetry was found within at least one part of the surgical ROI.

Histopathological Validation

After classical hematoxylin and eosin staining, FCDs were histopathologically confirmed by a neuropathologist with expertise in epilepsy pathology (*_blinded for review_*, 20 years of experience), and classified according to International League Against Epilepsy classification.²⁰

Statistical Analysis

Statistical analyses were performed by using ad hoc routines implemented in R 3.3.3 software.²¹

For each individual patient, we compared the BOLD metrics (ReHo, ALFF, fALFF, and DC) and PET-SUV values before resection of the ipsilateral with contralateral ROIs using absolute values and lateralization index ($[(\text{Ipsilateral} - \text{Contralateral}) / ((\text{Ipsilateral} + \text{Contralateral}))]$).²² Lateralization index is scaled between 0 and 1, where 0 reflects a symmetrical metric and the closer to 1 the more asymmetrical the metric. We assessed the significance of the lateralization index of all the patients using one-sample Wilcoxon test, using a reference value of 0. Potential correlations of lateralization indices of SUV and BOLD metrics over the patients were evaluated using Spearman's correlation.

To compare BOLD metrics lateralization of patients and controls in the same ROIs, we used Z-scores of lateralization indexes of the patients, relative to the mean and standard deviation of lateralization indexes from control group in the same ROIs. A Z-score higher than 1.96 or lower than -1.96 was considered as significant.

Results

Included Patients

Eighteen consecutive patients were evaluated for inclusion and had fMRI. After multidisciplinary evaluation, 10 patients had surgery, 8 of them after stereo-electroencephalographic

analysis. Among the 10 patients, 3 had to be excluded because BOLD images displayed too many motion artifacts ($n = 2$, displacements larger than 2 mm during the whole fMRI sequence) and because no FCD was confirmed in the histologic examination ($n = 1$).

Finally, seven patients were included (4 girls) for the study, with a median age of 9 years (range: 3–15 years). Clinical data are listed in ► **Supplementary Table S1** (available in the online version). One patient (patient 1, aged 3) had to be sedated using melatonin. The other patients were resting but not sleeping during the acquisition, as checked on the concurrent EEG. No correlation was found between clinical data (FCD localization, subtype, resected volume, age, epilepsy duration, antiepileptic drugs) and fMRI metrics. After structural imaging review, three patients had subtle focal abnormalities that were not described previously (blurring of the gray matter–white matter junction [$n = 2$], abnormal sulcation [$n = 1$], see ► **Table 1**).

Six healthy controls (2 girls) were included, with a median age of 11 years (range: 6–17 years). No structural MRI abnormality was found in the controls.

Regional Homogeneity

ReHo lateralization indices were positive in 4/7 patients due to a higher value in the surgical ROIs than the contralateral side

Table 1 Visual analysis of structural and functional imaging data of the included patients ($n = 7$)

Patient number	Structure imaging abnormalities	PET SUV map	ReHo map	DC map
1	None	Larger surgical ROI Slight hypometabolism in the upper part of the surgical ROI	Larger surgical ROI Increase in the upper part of the surgical ROI	Larger surgical ROI Increase in the upper part of the surgical ROI
2	None	Larger surgical ROI Slight hypometabolism in the upper part of the surgical ROI	Inconclusive Slight diffuse increase in the ROI without focal abnormality	Larger surgical ROI Focal increase in the medial part of the ROI
3	Abnormal sulcation Blurred gray matter–white matter junction	Larger PET abnormality Strong focal hypometabolism larger than the resected area	Larger surgical ROI Focal strong increase in half of the ROI	Inconclusive Slight diffuse increase of DC in the ROI
4	Blurred gray matter–white matter junction	Larger PET abnormality Focal hypometabolism larger than the resected area	Larger ReHo high value Focal increase concordant with PET hypometabolism	Inconclusive No visible focal abnormality
5	None	Larger surgical ROI Ill-defined hypometabolic area in the upper part of the surgical ROI	Inconclusive Slight increase in the upper part of the surgical ROI	Inconclusive No visible focal abnormality
6	Blurred gray matter–white matter junction	Larger surgical ROI Focal hypometabolism concordant with structural abnormality	Larger surgical ROI Focal increase concordant with structural and PET abnormalities	Inconclusive Slight decrease of DC in the area of structural and PET abnormalities
7	None	Full colocalization Focal hypometabolism	Inconclusive Diffuse decrease in the ROI without focal abnormality	Inconclusive Slight increase in the middle of the ROI

Abbreviations: ALFF, amplitude of low frequency fluctuation; BOLD, blood oxygenation level dependent; DC, degree centrality; fALFF, fractional ALFF; ReHo, regional homogeneity; PET, positron emission tomography; ROI, region of interest.

ALFF and fALFF maps did not show any visible focal abnormality concordant with surgical ROI or PET hypometabolism. Larger surgical ROI was defined as focal BOLD/PET abnormality found within a larger surgical ROI. Larger BOLD/PET abnormality was defined as focal abnormality overlapping the surgical ROI and the surrounding brain. Inconclusive was defined as no clear focal BOLD/PET asymmetry within at least one part of the surgical ROI.

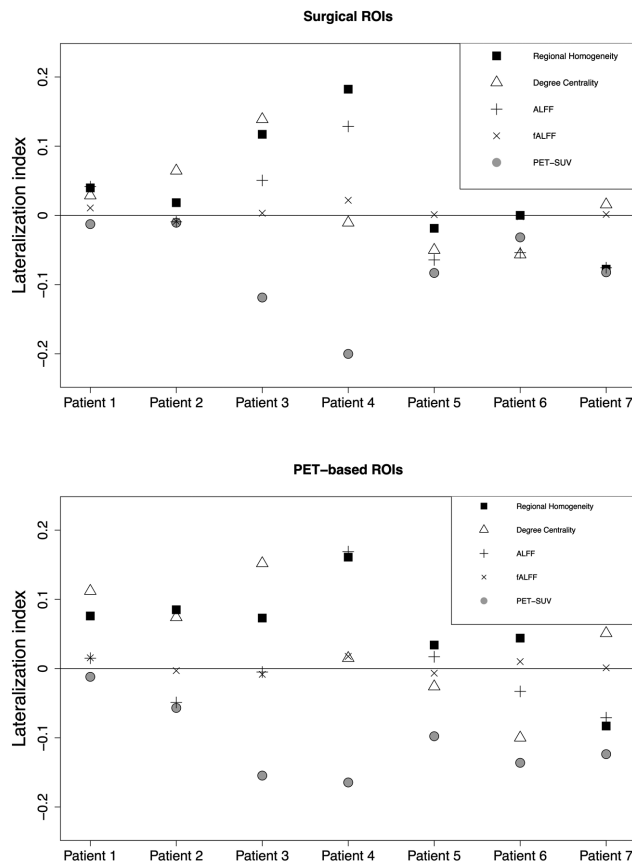


Fig. 1 Lateralization indices of regional homogeneity, degree centrality, amplitude of low frequency fluctuations, fractional amplitude of low frequency fluctuation (ALFF) and fluorodeoxyglucose-positron emission tomography (FDG-PET). Standardized uptake value between the focal cortical dysplasia resected area (upper graph) or the PET-based region of interest (ROI; lower graph) and the contralateral sulci. fALFF, fractional ALFF; SUV, standardized uptake value.

area (→ Fig. 1, → Supplementary Tables S2-S4, available in the online version), among them 3/7 lateralization indices being significantly higher than in controls (Z-scores between 1.96 and 2.52, → Fig. 2). Using PET-based ROIs, 6/7 lateralization indices were positive (1/7 being significantly higher than in controls [Z-score 2.92], and 3/7 having a Z-score between 1.05 and 1.86). However, one patient (patient 7, frontal mesial small-sized type IIb FCD) had negative lateralization indices using both surgical and PET-based ROIs (Z-score -2.08 and -1.81 , respectively). Therefore, the median lateralization index of all the patients was not significantly higher than 0 for surgical ROIs ($p = 0.23$), even if there was a trend using PET-based ROIs ($p = 0.08$).

Other BOLD Metrics (DC, ALFF, and fALFF)

No significant lateralization among all the patients was seen using DC, ALFF, and fALFF (→ Fig. 1). Lateralization indices were inconsistently positive or negative, not modified when PET-based ROIs were used. No significant correlation was found between different BOLD metrics lateralization indices.

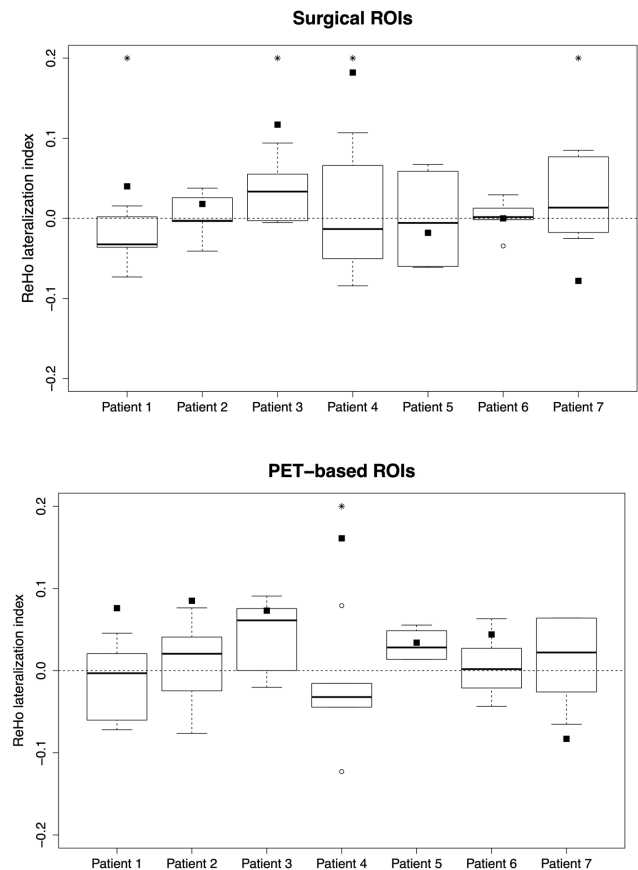


Fig. 2 Boxplots of regional homogeneity (ReHo) lateralization indices of controls. Each box represents the lateralization indices of the controls within the region of interest (ROI) of each patient (upper graph: surgical ROI, lower graph: positron emission tomography [PET]-based ROI). Black squares indicate the ReHo lateralization indices of the patients. * indicates when lateralization index of the patient is significantly different from the controls (Z-score > 1.96).

Correlation with PET

FDG-PET SUVs of surgical ROIs were consistently lower in FCD area in comparison with contralateral area (lateralization indices median -0.087 , $p = 0.008$).

The two patients (patients 3 and 4) with the lowest PET lateralization indices also had the highest ReHo lateralization indices. However, no significant correlation was found between PET and BOLD metrics lateralization indices.

Visual Analysis of BOLD or PET Maps (→ Table 1, → Figs. 3 and 4)

PET SUV maps showed focal hypometabolism areas that were larger than the surgically removed areas in 4/7 patients, smaller in 2/7 and comparable in 1/7.

Visual analysis of the ReHo maps showed a focal increase of ReHo in at least one part of the resected area in 4/7 patients. Among these, the three patients with subtle structural abnormalities had focal ReHo increase that was spatially concordant with these signal changes. ReHo increase was also colocalized with PET hypometabolic areas in these four patients. ReHo visual analysis was considered inconclusive in the remaining

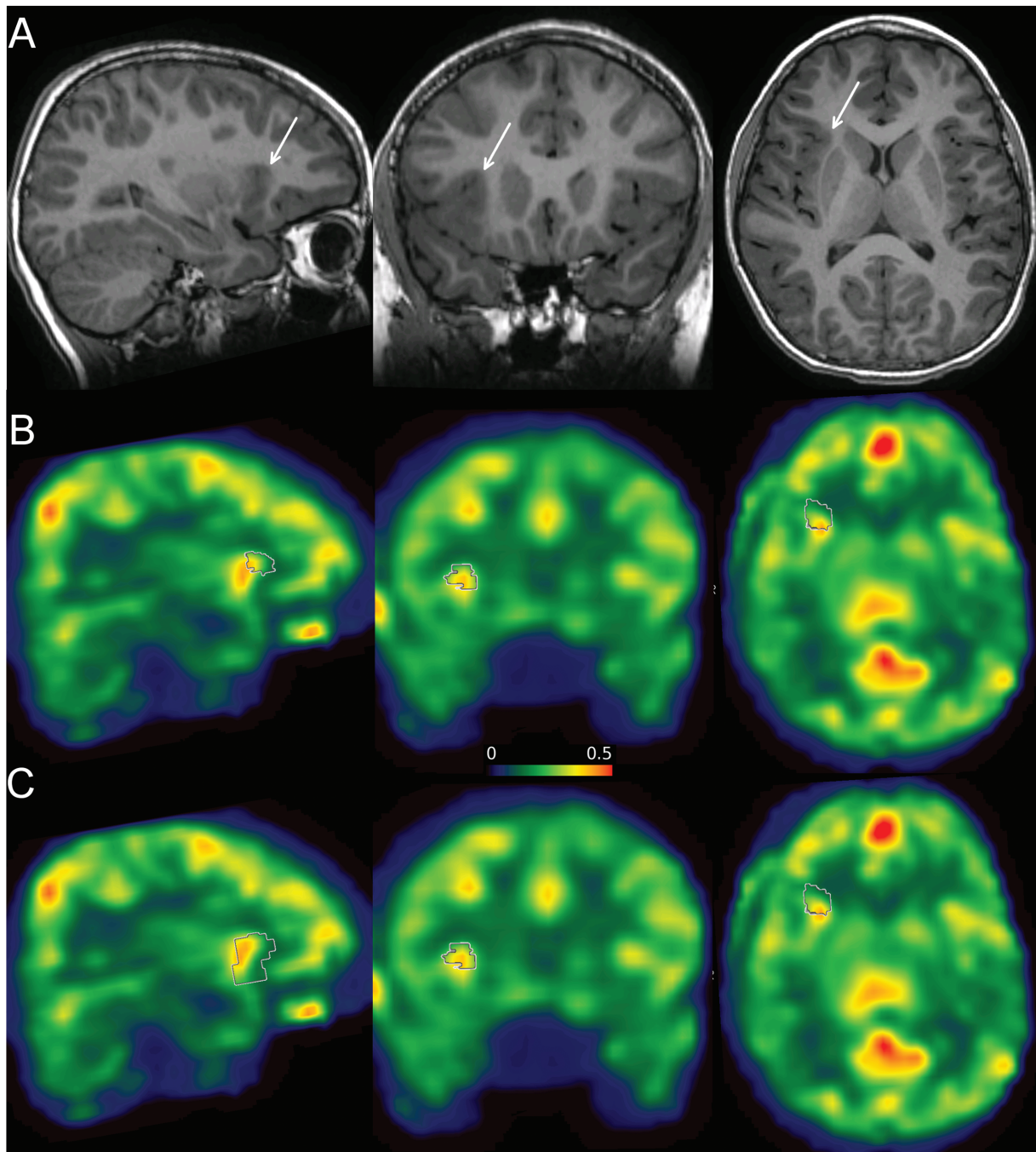


Fig. 3 Lateralization of regional homogeneity (ReHo) in patient 4 (9 years old girl). (A) Preoperative T1-weighted image (sagittal, coronal, and axial planes), showing a subtle white matter-gray matter blurring (white arrows). (B, C) Preoperative ReHo maps (sagittal, coronal, and axial planes, color scale represents Kendall's coefficients of concordance) with planned to be resected region of interest (ROI; white contours in B) and positron-emission tomography (PET)-based ROI (white contours in C). Resected volume matches with a part of the high ReHo volume, whereas PET-based ROI almost entirely matches with the high ReHo volume.

3/7 patients, because the increase/decrease in ReHo within the ROI was diffuse and moderate, not visually detectable without knowledge of the resected area.

DC maps visual analysis did not yield any significant information, because visible variations were moderate and vary among patients (increase/decrease).

ALFF and fALFF maps appeared rather useless in this context, because no consistent visual variations were observed.

Discussion

We report initial asymmetry results in spontaneous BOLD fluctuation metrics in surgically proven MRI-inconclusive FCD in children. We found that ReHo was in a substantial fraction of the pediatric patients higher in FCD area than in the contralateral area, yet not significantly, and that visual inspection revealed that these results were spatially

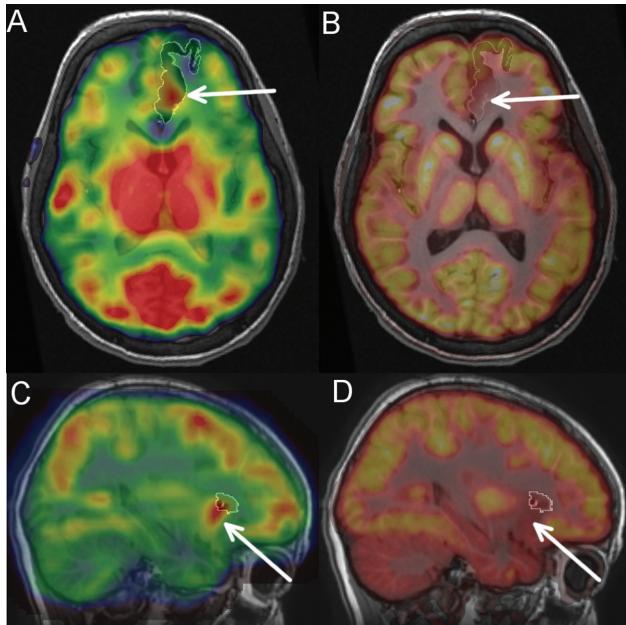


Fig. 4 Spatial relation between surgical and positron-emission tomography (PET)-based region of interests (ROIs). Regional homogeneity (ReHo) maps (A, C) and standardized uptake value (SUV) maps (B, D) overlaid on T1 preoperative images, with area of surgery delineated using white contours. Arrows indicate the hypometabolic regions on PET. In patient 6 (axial plane in A, B), the resected region is much larger than the PET hypometabolic area. The PET hypometabolic area (sought to match the focal cortical dysplasia area) is characterized by a higher ReHo and lower SUV than the whole ROI. In patient 4 (sagittal plane in C, D), the resected region is smaller than the PET hypometabolic area, to decrease the risk of postsurgical deficits. Consequently, the resected region does not include the whole area of high ReHo and low SUV.

correlated with structural abnormalities when present and hypometabolism area using FDG-PET.

Previously, Gupta et al¹³ reported in 14 adult patients with MRI-visible FCDs that ReHo was higher in FCDs than in the contralateral homotopic cortex and healthy controls. Our results support that these results may be extended to FCDs in children, even when MRI structural changes are absent or subtle. Three patients in our cohort had subtle MRI abnormalities within the FCD, which were seen *a posteriori*. These three patients also had the most obvious changes using ReHo maps. This suggests that high ReHo focus is more frequent when structural abnormalities are seen. This needs to be further assessed using larger cohorts. One patient (patient 7) had discordant results with lower ReHo in the FCD area. It was a small-sized frontal mesial type IIb FCD. These size/localization/type characteristics were also associated with misleading location using PET.²³ As investigated by Chen et al,¹⁴ higher ReHo areas could be used to help to detect epileptogenic zone in combination with other techniques, as none of existing techniques gives perfect sensitivity and specificity.

DC, ALFF, and fALFF had a lower yield than ReHo, as they provided no consistent variation among our patients. To our knowledge, no other study reported DC variation in FCDs. Using a different approach, Pedersen et al²⁴ reported that

several brain areas display common ReHo and DC variation in focal epilepsy patients, regardless of the FCD area. They also reported that ReHo and DC were positively correlated, a result we did not find in our FCD cohort. For the activity amplitude metrics, that is, ALFF and fALFF, we found no consistent effect between the FCD area and contralateral cortex, in contrast with the study of Gupta et al¹³ in adult patients. However, our study included children who were surgically treated with MRI-inconclusive FCDs, which may explain different results.

Pathophysiological Mechanisms

ReHo is thought to be linked to local synchronization of spontaneous fluctuations associated with neural activity in terms of neurovascular coupling that is spatially coherent at the millimeter scale.²⁵ Therefore, it may be higher in epileptogenic lesions, since these are characterized by rhythmic neuronal synchronization.¹ However, note that the time scale of this synchronization is very different using EEG (around 2–50 Hz) than for resting-state BOLD fMRI (0.01–0.1 Hz). Our results may suggest that the synchronization in FCD may be found using these different time scales due to the neurovascular coupling, possibly reflecting different features of the same underlying pathophysiological mechanism.

The lack of usable results for the amplitudes of the BOLD fluctuations, that is, ALFF and fALFF, can appear surprising, since FCDs have different neuronal activity than healthy tissue and we may hypothesize a different neurovascular coupling. However, abnormalities in EEG recordings cannot easily be transformed into deviations of the much slower low frequency BOLD oscillations, and to our knowledge, no other report has studied this issue in focal epileptogenic lesions.

We studied PET SUV lateralization in the same areas than fMRI metrics and found that high ReHo values were colocalized with hypometabolic areas. However, such a result should not be interpreted as a direct correlation between these fMRI metrics and FDG uptake. On the opposite, Nugent et al²⁶ reported that in a whole brain analysis on healthy subjects, PET-based regional metabolic rate of glucose was positively correlated with ALFF and ReHo. In our results, low FDG uptake is thought to reflect hypometabolism caused by an abnormal cortex in FCDs,⁷ whereas the higher ReHo reflects the higher local synchronicity, even if metabolic activity is lower.

Clinical Use

We performed an exploratory study to assess if ReHo is asymmetrical in a known epileptic focus. To pursue towards clinical use of higher ReHo areas, further studies still have to explore in a data-driven manner if ReHo maps allow the detection of an abnormality that will be confirmed by another technique (surgery or other imaging), eventually. Using a data-driven approach, several authors explored the ability of independent component analysis of resting-state-fMRI data to detect seizure onset zones.^{8,9,27–29} They found a good spatial localization of epileptic focus that allowed to predict surgical outcome.⁸ However, independent components categorization needs interpretation of aberrant

networks by experts,⁹ which is likely more complicated than analysis of ReHo maps that reveal targeted BOLD signatures. Their approach is based on network-derived data, while ReHo reflects localized BOLD fluctuations.

Resting-state fMRI may be useful in clinical practice since it does not need any ionizing radiation, contrast media injection nor significant cooperation of the child, except laying still in the MR magnet. The 10 minutes duration of the acquisition is longer than clinically used sequences but remains acceptable in a clinical workflow for these patients where the clinical impact may be high. Further studies should assess if shorter acquisitions may be sufficient. Thanks to dedicated toolboxes,¹⁵ the processing remains feasible in a clinical setting in terms of time and processing knowledge for neuroimaging-dedicated radiologists.

Study Considerations

Our study has several limitations, including the small size of our sample. This was caused by the rarity of such a population including MRI-negative FCD pediatric patients with surgical confirmation, which allowed a sound gold standard. In particular, we were unable to assess properly the influence of the FCD subtype, which could have a great influence. Type IIB FCDs seemed to have negative results, but it was based only on two patients, one of them having high ReHo focus. Further studies with larger samples may allow other analyses including the influence of FCD subtype, localization, intrinsic hemispheric asymmetries of spontaneous fluctuations, or the drugs used.

Second, the choice of the gold standard to delineate FCDs is very complicated in MRI-negative FCDs. We chose to use the resected area confirming the diagnosis of FCD as a reference standard, because it provides a sounder ground truth than clinical consensus (based on seizures semiology, EEG, and imaging) in these MRI-negative patients. Nevertheless, this reference standard is hampered by the imperfect colocalization of the whole FCD and the whole resected area: the FCD may be larger if the resection is limited by surgical risk, whereas the resected area may be larger than the FCD, if the FCD area is deeply localized and justifies a larger cortectomy to get surgical access. Therefore, it can affect our results because the effect may be diluted by the averaging of ReHo values within a ROI including healthy cortex. This prompted us to also investigate PET-based ROI in the same lobe as the proved FCD to assess if colocalization would be better. This method is not flawless, as PET hypometabolic area may be larger than the FCD.⁷ That is why we delineated ROIs using the lowest SUV areas. Using this technique, we found higher ReHo lateralization indices and good spatial correlation, supporting the relevance of high ReHo areas to help to detect FCDs. However, we did not delineate the whole epileptogenic zone in the ROIs of all the patients, since three of them were not seizure free after surgery.

Finally, we report here a combination of quantitative and qualitative analyses using lateralization indices and visual analysis, because of the small size of our sample. This work was intended to explore preliminary results in patients with confirmed FCD and further studies will be needed to assess relevant lateralization thresholds. Furthermore, the analysis

of lateralization precludes the ability from assessing whether the abnormality is in the FCD area and/or in the contralateral cortex. However, in a clinical context, the lateralization of the epileptic focus is most often known and the comparison of the two sides may be useful.

Conclusion

Our exploratory study indicates that regionally targeted resting-state fMRI derived metrics tend to be different in MRI-negative FCDs compared to the contralateral brain, particularly an increase in regional homogeneity of the BOLD signature was observed. These results need to be assessed in larger samples using a data-driven approach to explore their potential yield in FCD detection in a clinical context.

Funding

This work was funded by the Alain Rahmouni research grant from the French Society of Radiology.

Conflict of Interest

V.D.-R. was partially funded by GE Healthcare. Other authors have no relevant conflict of interest to disclose.

References

- 1 Wong-Kisiel LC, Blauwblomme T, Ho ML, et al. Challenges in managing epilepsy associated with focal cortical dysplasia in children. *Epilepsy Res* 2018;145:1–17
- 2 Blumcke I, Spreafico R, Haaker G, et al; EEBB Consortium. Histopathological findings in brain tissue obtained during epilepsy surgery. *N Engl J Med* 2017;377(17):1648–1656
- 3 Jayalakshmi S, Nanda SK, Vooturi S, et al. Focal cortical dysplasia and refractory epilepsy: role of multimodality imaging and outcome of surgery. *AJNR Am J Neuroradiol* 2019;40(05):892–898
- 4 Colombo N, Tassi L, Deleo F, et al. Focal cortical dysplasia type IIa and IIb: MRI aspects in 118 cases proven by histopathology. *Neuroradiology* 2012;54(10):1065–1077
- 5 Wilmshurst JM, Gaillard WD, Vinayan KP, et al. Summary of recommendations for the management of infantile seizures: task force report for the ILAE commission of pediatrics. *Epilepsia* 2015;56(08):1185–1197
- 6 Zijlmans M, Zweiphenning W, van Klink N. Changing concepts in presurgical assessment for epilepsy surgery. *Nat Rev Neurol* 2019;15(10):594–606
- 7 Chassoux F, Rodrigo S, Semah F, et al. FDG-PET improves surgical outcome in negative MRI Taylor-type focal cortical dysplasias. *Neurology* 2010;75(24):2168–2175
- 8 Boerwinkle VL, Cediell EG, Mirea L, et al. Network-targeted approach and postoperative resting-state functional magnetic resonance imaging are associated with seizure outcome. *Ann Neurol* 2019;86(03):344–356
- 9 Boerwinkle VL, Mohanty D, Foldes ST, et al. Correlating resting-state functional magnetic resonance imaging connectivity by independent component analysis-based epileptogenic zones with intracranial electroencephalogram localized seizure onset zones and surgical outcomes in prospective pediatric intractable epilepsy study. *Brain Connect* 2017;7(07):424–442
- 10 Zang Y, Jiang T, Lu Y, He Y, Tian L. Regional homogeneity approach to fMRI data analysis. *Neuroimage* 2004;22(01):394–400
- 11 Yang H, Long XY, Yang Y, et al. Amplitude of low frequency fluctuation within visual areas revealed by resting-state functional MRI. *Neuroimage* 2007;36(01):144–152

- 12 Zuo XN, Ehmke R, Mennes M, et al. Network centrality in the human functional connectome. *Cereb Cortex* 2012;22(08):1862–1875
- 13 Gupta L, Hofman PAM, Besseling RMH, Jansen JFA, Backes WH. Abnormal blood oxygen level-dependent fluctuations in focal cortical dysplasia and the perilesional zone: initial findings. *AJNR Am J Neuroradiol* 2018;39(07):1310–1315
- 14 Chen Z, An Y, Zhao B, et al. The value of resting-state functional magnetic resonance imaging for detecting epileptogenic zones in patients with focal epilepsy. *PLoS One* 2017;12(02):e0172094
- 15 Chao-Gan Y, Yu-Feng Z. DPARSF: a MATLAB toolbox for “Pipeline” data analysis of resting-state fMRI. *Front Syst Neurosci* 2010;4:13
- 16 Song XW, Dong ZY, Long XY, et al. REST: a toolkit for resting-state functional magnetic resonance imaging data processing. *PLoS One* 2011;6(09):e25031
- 17 Yan CG, Wang XD, Zuo XN, Zang YF. DPABI: data processing & analysis for (Resting-State) brain imaging. *Neuroinformatics* 2016;14(03):339–351
- 18 Wang X, Jiao D, Zhang X, Lin X. Altered degree centrality in childhood absence epilepsy: a resting-state fMRI study. *J Neurol Sci* 2017;373:274–279
- 19 Warbrick T, Rosenberg J, Shah NJ. The relationship between BOLD fMRI response and the underlying white matter as measured by fractional anisotropy (FA): a systematic review. *Neuroimage* 2017;153:369–381
- 20 Blümcke I, Thom M, Aronica E, et al. The clinicopathologic spectrum of focal cortical dysplasias: a consensus classification proposed by an ad hoc Task Force of the ILAE Diagnostic Methods Commission. *Epilepsia* 2011;52(01):158–174
- 21 R Core Team (2022). R: A language and environment for statistical computing. R Foundation for Statistical Computing, Vienna, Austria. <https://www.R-project.org/>
- 22 Leach JL, Awwad R, Greiner HM, Vannest JJ, Miles L, Mangano FT. Mesial temporal lobe morphology in intractable pediatric epilepsy: so-called hippocampal malrotation, associated findings, and relevance to presurgical assessment. *J Neurosurg Pediatr* 2016;17(06):683–693
- 23 Desarnaud S, Mellerio C, Semah F, et al. ¹⁸F-FDG PET in drug-resistant epilepsy due to focal cortical dysplasia type 2: additional value of electroclinical data and coregistration with MRI. *Eur J Nucl Med Mol Imaging* 2018;45(08):1449–1460
- 24 Pedersen M, Curwood EK, Vaughan DN, Omidvarnia AH, Jackson GD. Abnormal brain areas common to the focal epilepsies: multivariate pattern analysis of fMRI. *Brain Connect* 2016;6(03):208–215
- 25 Jiang L, Zuo XN. Regional homogeneity: a multimodal, multiscale neuroimaging marker of the human Connectome. *Neuroscientist* 2016;22(05):486–505
- 26 Nugent AC, Martinez A, D’Alfonso A, Zarate CA, Theodore WH. The relationship between glucose metabolism, resting-state fMRI BOLD signal, and GABAA-binding potential: a preliminary study in healthy subjects and those with temporal lobe epilepsy. *J Cereb Blood Flow Metab* 2015;35(04):583–591
- 27 Hunyadi B, Tousseyn S, Dupont P, Van Huffel S, De Vos M, Van Paesschen W. A prospective fMRI-based technique for localising the epileptogenic zone in presurgical evaluation of epilepsy. *Neuroimage* 2015;113:329–339
- 28 Thornton RC, Rodionov R, Laufs H, et al. Imaging haemodynamic changes related to seizures: comparison of EEG-based general linear model, independent component analysis of fMRI and intracranial EEG. *Neuroimage* 2010;53(01):196–205
- 29 Zhang CH, Lu Y, Brinkmann B, Welker K, Worrell G, He B. Lateralization and localization of epilepsy related hemodynamic foci using presurgical fMRI. *Clin Neurophysiol* 2015;126(01):27–38